Proceedings of IMECE '03
2003 ASME International Mechanical Engineering Congress and Exposition
November 15-21, 2003, Washington, D.C. USA

IMECE2003-41966

CYCLE-TO-CYCLE CONTROL OF HCCI ENGINES

Gregory M. Shaver

Design Division
Dept. of Mechanical Engineering
Stanford University
Stanford, California 94305-4021
Email: shaver@stanford.edu

J.Christian Gerdes

Design Division
Dept. of Mechanical Engineering
Stanford University
Stanford, California 94305-4021
Email: gerdes@cdr.stanford.edu

ABSTRACT

With stated benefits ranging from increased thermal efficiency to significantly reduced NO_x emissions, Homogeneous Charge Compression Ignition (HCCI) represents a promising combustion strategy for future engines. When achieved by reinducting exhaust gas with a variable valve actuation (VVA) system, however, HCCI possesses nonlinear cycle-to-cycle coupling through the exhaust gas and lacks an easily identified trigger comparable to spark or fuel injection. This makes closed-loop control decidedly nontrivial. To develop a controller for HCCI, the engine cycle is partitioned into five stages: adiabatic, constant pressure induction of re-inducted product and reactant charge; isentropic compression to the point just prior to combustion initiation; constant volume combustion; isentropic expansion of product gases; isentropic exhaust of product gases. Using this framework, a nonlinear low-order model of HCCI combustion is formulated, where the input is the molar ratio of reinducted products to fresh reactants and the output is the peak in-cylinder pressure. Comparison with experimental in-cylinder pressure data shows that the model, while simple, offers reasonable fidelity. Using the nonlinear model, a linearized model and an accompanying LQR controller are formulated and implemented on a more detailed model presented in previous work. Results from these simulations show that the modeling and control approach is indeed successful at tracking a varying desired work output while maintaining a constant desired combustion phasing.

NOMENCLATURE

$P_i(k)$	Pressure following stage i for engine cycle k
$\beta_i(k)$	Normalized peak pressure for engine cycle k
$T_i(k)$	Temperature following stage i for engine cycle k
V_i	Cylinder volume following stage i
$\alpha(k)$	Proportion of moles of reinducted exhaust to moles of reactant at engine cycle k
ϕ	Equivalence ratio
H	Total enthalpy[kJ]
U	Total internal energy [kJ]
N_i	Number of moles of species i or state i
$\bar{h}_i$	Molar enthalpy of species i [kJ/mol]
$\bar{c}_{p,i}$	Specific heat of species i [kJ/K mol]
$\Delta_f \bar{h}_i$	Molar heat of formation of species i [kJ/mol]
K	LQR controller gain
χ	Exhaust manifold heat loss coefficient
η	In-cylinder heat loss coefficient
T_{ref}	Reference temperature [K]
T_{inlet}	Temperature of incoming reactant species [K]
γ	Specific heat ratio
R_u	Universal gas constant
V_{inlet}	Inducted volume through intake
N_r	Number of moles of reactant charge inducted through intake
N_p	Number of moles of product from previous cycle inducted through exhaust
P_{atm}	Atmospheric pressure

T_{atm} Atmospheric temperature
IVO Intake valve opening position [degrees]
EVC Exhaust valve closing position [degrees]
IVC Intake valve closing position [degrees]
EVO Exhaust valve opening position [degrees]
$\bar{}$ Steady state value
$\tilde{}$ Deviation from steady state value

1 Introduction

Homogeneous charge compression ignition (HCCI) holds great promise as a means to reduce NO_x emissions in internal combustion engines (Caton *et al.* 2003). HCCI is achieved by increasing the sensible energy of a well mixed reactant charge, allowing ignition to occur by compression alone. This leads to a low post-combustion temperature, which significantly reduces NO_x emissions. There are several methods to initiate HCCI, such as heating or pre-compressing the intake air (Tunestal *et al.* 2001, Martinez-Frias *et al.* 2000), varying the compression ratio (Christensen *et al.* 1999) or modulating intake and exhaust flows using variable valve actuation (VVA) (Caton *et al.* 2003, Law *et al.* 2001, Kaahaaina *et al.* 2001). Using the VVA system, products exhausted during the previous cycle are re-inducted and mixed with fresh charge, resulting in the required increase in reactant gas sensible energy.

Regardless of the method chosen, however, HCCI combustion exhibits some fundamental control challenges concerning combustion phasing and work output. Unlike spark ignition (SI) or diesel engines, where the combustion is initiated via spark and fuel injection, respectively, HCCI has no specific event that initiates combustion. Therefore, ensuring that combustion occurs with acceptable timing, or at all, is more complicated than in the case of either SI or diesel combustion. Combustion phasing in HCCI is dominated by chemical kinetics, which depends on the in-cylinder concentrations of reactants and products, their temperature and when they are allowed to begin mixing. Work output is dependent on both the combustion phasing and the amount of reactant species present in the cylinder. Thus to control HCCI achieved with VVA it is essential to understand how the valves influence mass flows and combustion phasing and how previous combustion cycles influence the temperature of the reinducted products.

The ability to phase HCCI and control work output on the system studied is a direct consequence of being able to vary the valve timings with the VVA system. The current approach taken is to leave the intake valve closing (IVC) and exhaust valve opening (EVO) times fixed and modulate the exhaust valve closing (EVC) and intake valve opening (IVO) times to control mass flows. If the desired result of valve motion is to induct a certain ratio of re-inducted products to fresh reactants, IVO and EVC are to some extent redundant. Any desired ratio can be achieved through an infinite number of combinations of IVO and EVC. In addition to its role in determining this ratio, however, IVO also determines when the reactant and re-inducted product gases begin to mix. This, in turn, influences combustion timing through the chemical kinetics. While the exact kinetics are quite complex, a simplified Arrhenius rate expression captures experimental data quite well (Shaver *et al.* 2003) and offers a very simple understanding of the process. In short, given two mixtures with identical ratios of re-inducted products and reactants at the same temperature, early IVO leads to a greater residence time in the cylinder and earlier phasing of combustion. In this way, both desired phasing and peak pressure can be controlled simultaneously by varying IVO and EVC. Here desired phasing is assumed to be constant and the control problem then becomes how to vary IVO and EVC to achieve this phasing while tracking a changing load on a cycle-to-cycle basis.

To synthesize a controller capable of this task, the system model used must capture the cycle to cycle interactions arising from the fact that the temperature of the re-inducted exhaust gases depends upon the previous combustion event. In ongoing work (Shaver *et al.* 2003, Shaver *et al.* 2004), a higher order (10-state) model of HCCI combustion has been formulated, showing very good correlation with experimental combustion phasing and in-cylinder pressure values as the engine cycle evolves. This paper outlines a highly simplified version of this model for constant speed operation that focuses on the evolution of the peak cylinder pressure (which is directly related to work output at constant phasing). Since the molar ratio of re-inducted products to fresh reactants can be controlled through some combination of IVO and EVC while leaving phasing constant, this ratio is chosen as the input of the model.

This low-order model is formulated by discretizing the various processes which occur during a HCCI combustion engine cycle, then linking them together. A map from the desired in-cylinder ratio of fresh reactant charge and re-inducted products to the required IVO and EVC valve timing is then realized through simulation of the induction process. Together, the model relating composition with peak pressure and the map from desired composition to VVA valve timing complete the mathematical description of HCCI combustion achieved through the use of VVA. The model is then linearized about an operating point and used to synthesize an LQR control law. Implemented on the 10-state model, this control law is able to successfully control both combustion phasing and peak pressure, therefore indirectly controlling work output. The results are very promising, suggesting that the controller synthesis strategy developed in this work is a very good candidate for future experimental implementation.

2 Modeling Approach

The framework for modeling HCCI combustion in a simple way involves partitioning the engine cycle into five stages:

1. Mixing of reactant and re-inducted product gases during a constant pressure, adiabatic induction process
2. Isentropic compression to the point where combustion initiates
3. Constant volume combustion to major products
4. Isentropic expansion to the point where the exhaust valve opens
5. Isentropic expansion through the exhaust valve.

In order to facilitate this, the thermodynamic state of the system at several points is tracked, as shown in Figure 1. The first

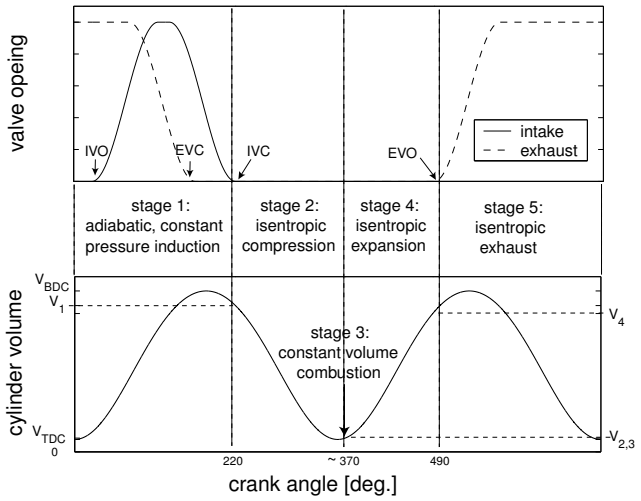

Figure 1. General view of partitioned HCCI cycle

thermodynamic state considered follows the stage 1 induction process, which occurs at the intake valve closing (IVC) location. At this point the reactant charge and re-inducted product gases are assumed to be homogeneously mixed throughout the combustion chamber. During stage 2, isentropic compression is assumed. The thermodynamic state of the system is expressed at the end of this stage and is related directly to the post-induction condition following the induction stage. Constant volume combustion is then assumed during stage 3 at a fixed combustion phasing, producing the major products of combustion at an elevated temperature and pressure. The thermodynamic state at this point is evaluated with respect to the previous ones. Heat transfer during the constant volume combustion stage is included to approximate the total amount of in-cylinder heat transfer that occurs during the engine cycle. The assumption that the combustion event phasing occurs at a consistent point just past top dead center is motivated by previous experimental work which shows that as long as the IVO and EVC timings lie along a particular linear map the combustion phasing is relatively constant. This will be discussed in more detail in Section 7. Post-combustion, the stage 4 expansion process is assumed isentropic. It progresses until exhaust valve opening (EVO) occurs. The major product gases are then assumed to exhaust isentropically to the exhaust manifold. The thermodynamic state of the system is evaluated at this point by assuming atmospheric pressure in the exhasut manifold. The re-inducted product temperature on the next cycle is then related to the fifth thermodynamic state temperature from the previous cycle. Note that at points between stages, the cylinder volume is known (see Figure 1), which is necessary information in linking the thermodynamic states of the system together. Following this method, a model of HCCI combustion can be formulated from a system input related to the composition of the inducted reactants and products and the system output, the peak pressure. It will be clear from this model that cycle-to-cycle dynamics are present due to the re-induction of product species from the previous cycle.

2.1 Instantaneous Mixing of Species

The low-order model of HCCI combustion presented in this paper relates the composition of gases inducted into the cylinder to the in-cylinder peak pressure. The ratio of the moles of re-inducted product to the moles of inducted reactant charge, defined as α, quantifies the composition of the in-cylinder gas prior to combustion. The low-order model will be formulated in such a way that α will be the input to the system. Using this definition of inducted gas composition, the mixing of the reactant and re-inducted product species during the induction process can be represented as:

$$\begin{gathered}\alpha(k)\,(3\phi CO_2+4\phi H_2O+18.8N_2+5(1-\phi)O_2)\\+(\phi C_3H_8+5O_2+18.8N_2)\rightarrow\\\phi C_3H_8+5((\alpha(k)(1-\phi)+1)O_2+18.8(1+\alpha(k))N_2+\\3\alpha(k)\phi CO_2+4\alpha(k)\phi H_2O\end{gathered}\tag{1}$$

where ϕ is the equivalence ratio, which is a measure of the relative amounts of fuel, C_3H_8, and oxidizer, air, in the reactant charge inducted through the intake.

The first law of thermodynamics applied during the induction process is:

$$\frac{d(mu)}{dt}=\dot{Q}_{induction}-\dot{W}+\dot{m}_{rct}h_{1,rct}+\dot{m}_{prod}h_{1,prod}\tag{2}$$

where the total internal energy in the cylinder is mu, the heat transfer during induction is $\dot{Q}_{induction}$, and the work due to the piston movement is $\dot{W}=p\dot{V}$. The reactant mass flow rate through the intake and re-inducted product mass flow rate through the exhaust are $\dot{m}_{rct}$ and $\dot{m}_{prod}$, with corresponding enthalpies in the intake and exhaust manifolds of $h_{1,rct}$ and $h_{1,prod}$. With the following assumptions:

1. no heat transfer during induction: $\dot{Q}_{induction} = 0$
2. constant in-cylinder pressure: $\dot{p} = 0$
3. intake and exhaust manifold conditions do not change during induction process

and the relation that $h = u + p\nu$:

$$\dot{m}_{prod} h_{1,prod} + \dot{m}_{rct} h_{1,rct} = \frac{d(mh)}{dt} \tag{3}$$

When this equation is integrated from the beginning to the end of the induction process with the assumption of manifold conditions not varying during induction, the resulting expression is:

$$\sum_{\substack{1 \\ products}} N_i \bar{h}_i(T_{1,prod}) + \sum_{\substack{1 \\ reactants}} N_i \bar{h}_i(T_{1,rct}) = \sum_{1} N_i \bar{h}_i(T_1) \tag{4}$$

where N_i is the number of moles of species i and $\bar{h}_i$ is the molar enthalpy of species i. Assuming that the molar enthalpy of species i can be approximated using a specific heat, $\bar{c}_{p,i}$ that is constant with temperature, then:

$$\bar{h}_i(T) = \Delta_f \bar{h}_i + \bar{c}_{p,i}(T - T_{ref}) \tag{5}$$

where $\Delta_f \bar{h}_i$ is the molar heat of formation of species i, and T_{ref} is the reference temperature corresponding to the heat of formation. Substitution of Equation 5 into Equation 4, applied to Equation 1 yields after rearrangement, the following:

$$T_1(k) = \frac{C_1 T_{inlet} + C_2 \alpha(k) T_{1,prod}(k)}{C_1 + C_2 \alpha(k)} \tag{6}$$

where:

$$C_1 = \phi \bar{c}_{p,C_3H_8} + 5\bar{c}_{p,O_2} + 18.8\bar{c}_{p,N_2} \tag{7}$$

$$C_2 = 3\phi \bar{c}_{p,CO_2} + 4\phi \bar{c}_{p,H_2O} + 18.8\bar{c}_{p,N_2} + 5(1-\phi)\bar{c}_{p,O_2} \tag{8}$$

The reinducted product species are assumed to have a temperature, $T_{1,prod}(k)$, that is directly related to the temperature of the exhausted products from the last cycle, $T_5(k-1)$, by the simple relation:

$$T_{1,prod}(k) = \chi T_5(k-1) \tag{9}$$

This simple relation is meant to represent heat transfer. More complex models of exhaust manifold heat transfer could be used, and likely would be needed for operation at various speeds. This expression, however, matches experimental observations reasonably well while keeping the relation as simple as possible. Substituting 9 into 6, leads to:

$$T_1(k) = \frac{C_1 T_{inlet} + C_2 \chi \alpha(k) T_5(k-1)}{C_1 + C_2 \alpha(k)} \tag{10}$$

2.2 Isentropic Compression to Pre-Combustion State

With the assumption that the compression stage occurs isentropically, the thermodynamic state of the system prior to and following the stage may be related with the following well known relations for an ideal gas:

$$T_2(k) = \left(\frac{V_1}{V_{2,3}}\right)^{\gamma - 1} T_1(k) \tag{11}$$

$$P_2(k) = \left(\frac{V_1}{V_{2,3}}\right)^{\gamma} P_{atm} \tag{12}$$

where γ is the specific heat ratio.

2.3 Constant Volume Combustion

In order to model HCCI combustion in a very simple way, it is assumed that the combustion reaction phase, from reactants to products, occurs instantaneously just past top dead center homogeneously throughout the piston chamber. This requires that the inducted reactants and products be mixed in such a way that combustion phasing remains constant, a point addressed later. The instantaneous combustion assumption is justified by the fact that HCCI combustion is typically very fast. It is further assumed that only major products result from the mixture of reactants at an equivalence ratio, ϕ, such that the combustion reaction can be written as:

$$\begin{gathered} \phi C_3H_8 + 5(\alpha(k)(1-\phi)+1)O_2 + 18.8(1+\alpha(k))N_2 \\ +3\phi\alpha(k)CO_2 + 4\alpha(k)\phi H_2O \rightarrow \\ (1+\alpha(k))(3\phi CO_2 + 4\phi H_2O + 18.8N_2 + 5(1-\phi)O_2) \end{gathered} \tag{13}$$

Since the system is closed during combustion (i.e. there are no flows into the system), the first law of thermodynamics during combustion is:

$$m\frac{du}{dt} = \dot{Q}_{combustion} - \dot{W} \tag{14}$$

The assumption that combustion occurs quickly implies that the volume change during combustion is negligible. In that case the

piston work term, $\dot{W} = p\dot{V}$, is approximately zero. The first law then becomes:

$$m\frac{du}{dt} = \dot{Q}_{combustion} \tag{15}$$

Integrating this expression results in:

$$U_2 = U_3 + Q_{combustion} \tag{16}$$

A model for the in-cylinder heat transfer during combustion is necessary. This is obtained by assuming that the total amount of heat transfer is a certain percentage of the chemical energy available from the combustion reaction:

$$Q_{combustion} = LHV_{C_3H_8} N_{C_3H_8} \varepsilon \tag{17}$$

where $LHV_{C_3H_8}$ is referred to as the lower heating value for propane, and is defined as:

$$LHV_{C_3H_8} = 3\Delta_f \bar{h}_{CO_2} + 4\Delta_f \bar{h}_{H_2O} - \Delta_f \bar{h}_{C_3H_8} \tag{18}$$

Substitution of the in-cylinder heat transfer model, Equation 17, into the internal energy equation, Equation 16, results in an expression for the post-combustion internal energy:

$$U_2 = U_3 + LHV_{C_3H_8} N_{C_3H_8} \varepsilon \tag{19}$$

which can then be expanded to:

$$\begin{gathered} \sum_2 N_i \bar{h}_i(T_2) - R_u T_2(k) \sum_2 N_i = \\ \sum_3 N_i \bar{h}_i(T_3) - R_u T_3(k) \sum_3 N_i + LHV_{C_3H_8} N_{C_3H_8} \varepsilon \end{gathered} \tag{20}$$

Applying the constant specific heat assumption, Equation 5, to the expanded form of the post-combustion internal energy expression, Equation 20, gives:

$$T_3(k) = \frac{C_4 + (C_1 + C_2\alpha(k))T_2(k)}{C_2(1+\alpha(k))} \tag{21}$$

where:

$$C_4 = (1-\varepsilon)(\phi LHV_{C_3H_8} + (C_2 - C_1)T_{ref}) \tag{22}$$

The in-cylinder pressure following the constant volume combustion stage, $P_3(k)$, can be related to the temperature at that point, $T_3(k)$, using the following derivation. The number of moles in the cylinder following the compression stage can be expressed by using the ideal gas law:

$$N_2 = \frac{P_2 V_{2,3}}{R_u T_2} \tag{23}$$

The number of moles in the cylinder following combustion, N_3, can be related to N_2 by inspection of Equation 13 by:

$$N_3 = \left(\frac{1+\alpha(k)}{f+\alpha(k)}\right) N_2 \tag{24}$$

where $f = 24.8/25.8$. The ideal gas law applied to state 3 gives:

$$P_3 = \frac{N_3 R_u T_3}{V_{2,3}} \tag{25}$$

Assembling Equations 23-25 with Equations 11 and 12, and solving for P_3 gives the following relation between temperature and pressure:

$$P_3(k) = \frac{1+\alpha(k)}{f+\alpha(k)} \left(\frac{V_1}{V_{2,3}}\right)^{\gamma} \frac{C_1 + C_2\alpha(k)}{C_2(1+\alpha(k))T_3(k) - C_4} P_{atm} T_3(k) \tag{26}$$

2.4 Isentropic Expansion

The fourth stage of HCCI is approximated as isentropic volumetric expansion following the constant volume combustion stage. This results in the relations for the thermodynamic state of the system following the expansion as:

$$T_4(k) = \left(\frac{V_{2,3}}{V_4}\right)^{\gamma-1} T_3(k) \tag{27}$$

$$P_4(k) = \left(\frac{V_{2,3}}{V_4}\right)^{\gamma} P_3(k) \tag{28}$$

2.5 Isentropic Expansion through the Exhaust Valve to Atmospheric Pressure

The exhaust stage is also assumed to be isentropic. With the additional assumption that the pressure in the exhaust manifold is atmospheric, the in-cylinder temperature following the expansion stage can be related to the temperature of the product gas following the exhaust stage:

$$T_5(k) = \left(\frac{P_{atm}}{P_4}\right)^{\frac{\gamma-1}{\gamma}} T_4(k) \tag{29}$$

3 Discrete Nonlinear Reduced-Order Pressure Equation

By linking the distinct processes which occur during HCCI combustion - combining Equations 10, 11, 21, 26, 27, 28 and 29 - a relation between the input to the system, α, and the post-combustion temperature can be realized:

$$T_{3,k} = \frac{C_4 + \left(\frac{V_{BDC}}{V(\theta_{c,k})}\right)^{\gamma-1} C_1 T_{inlet} + C_2 \chi \alpha_k \left(\frac{1+\alpha_{k-1}}{f+\alpha_{k-1}} \frac{C_1 + C_2 \alpha_{k-1}}{C_2(1+\alpha_{k-1})T_{3,k-1} - C_4}\right)^{\frac{1-\gamma}{\gamma}} T_{3,k-1}^{\frac{1}{\gamma-1}}}{C_2(1+\alpha_k)} \tag{30}$$

The presence of cycle-to-cycle dynamics is evident by inspection of Equation 30, as the current cycle peak temperature is related to that of the previous cycle.

In order to get the desired relationship between the input, α, and a measurable output (namely, peak pressure), Equations 26 and 30 can be combined to arrive at a closed loop system equation for the peak pressure, with α as the input. With the approximation that $(1+\alpha_k)/(f+\alpha_k) \approx 1$, this relation is:

$$P_k = \frac{c_1 + c_2\alpha_k}{1+\alpha_k} \frac{c_{12}(c_1 + c_2\alpha_{k-1}) + c_{13}P_{k-1}(1+\alpha_{k-1}) + c_{15}\chi\alpha_k P_{k-1}^{1/\gamma}}{c_{11}(c_1 + c_2\alpha_{k-1}) + c_{10}P_{k-1}(1+\alpha_{k-1}) + c_{14}\chi\alpha_k P_{k-1}^{1/\gamma}} \tag{31}$$

where:

$$c_5 = V_1/V_{2,3} \tag{32}$$

$$c_6 = c_4 + c_5^{\gamma-1} c_1 T_i \tag{33}$$

$$c_{10} = c_2^2(c_4 - c_6) \tag{34}$$

$$c_{11} = -c_5^{\gamma} P_{atm}(c_4 - c_6)c_2 \tag{35}$$

$$c_{12} = -c_6 c_5^{2\gamma} P_{atm}^2 \tag{36}$$

$$c_{13} = c_6 c_5^{\gamma} P_{atm} c_2 \tag{37}$$

$$c_{14} = -c_2^2 c_4 c_5^{\gamma-1} P_{atm}^{(\gamma-1)/\gamma} \tag{38}$$

$$c_{15} = c_5^{\gamma} P_{atm}^{(2\gamma-1)/\gamma} c_2 c_4 c_5^{\gamma-1} \tag{39}$$

4 Model Comparison with Experiment

With the large number of assumptions made in this modeling approach, a comparison with experimental results is necessary to gain confidence in the resulting model. A series of experiments at three different operating conditions were made on the single-cylinder research engine utilizing fully flexible variable valve actuation (VVA). Variations in operating condition were made by adjusting the exhaust valve closing (EVC) and intake valve opening (IVO) positions, effectively changing the ratio of re-inducted products and reactants. Figure 1 shows the general valve profile used on the research engine. Measurement of the in-cylinder pressure, p, is available on the research engine through the use of a pressure transducer. The average inlet air flow rate, $\bar{\dot{V}}$, is available by evaluating the pressure drop across a laminar flow element located on the inlet section. Additionally the exhaust temperature is measured using a thermocouple. The experimental values are given in Table 1 for each of three cases considered experimentally.

case	IVO/EVC	$\bar{\dot{V}}$ [$\frac{m^3}{s}$]	$T_{ex}[K]$	P_{max} [atm]
1	25/165	0.0039	697	59.5
2	45/185	0.0033	655	52.5
3	65/205	0.0026	638	44.5

Table 1. Experimentally monitored values

case	IVO/EVC	α	$T_1[K]$
1	25/165	0.64	501
2	45/185	0.89	512
3	65/205	1.29	535

Table 2. Estimated experimental Values

The total volume flow of reactant mixture through the intake during an engine cycle, V_{inlet}, is related to the average inlet air flow rate and the cycle time, t_{cycle}, by:

$$V_i = \bar{\dot{V}} t_{cycle} \tag{40}$$

With the assumption that the reactant charge is inducted under atmospheric conditions and behaves as an ideal gas, the total number of moles of reactant species is:

$$N_r = \frac{P_{atm} V_i}{R_u T_{atm}} \tag{41}$$

Using the ideal gas law for the mixture of products and reactants in the cylinder at state 1:

$$N_r \left(\frac{\alpha}{f} + 1\right) = N_p + N_r = N_{total} = \frac{P_{atm} V_1}{R_u T_1} \tag{42}$$

Utilizing the argument presented in Section 2.1 of constant pressure, adiabatic mixing of the reactants and re-inducted products, Equation 10, can be used:

$$T_1(k) = \frac{C_1(T_{inlet})T_{inlet} + C_2(T_{ex})\chi\alpha(k)T_{ex}}{C_1(T_1) + C_2(T_1)\alpha(k)} \tag{43}$$

Here the specific heats are allowed to vary with temperature to provide the most accurate expression of the first law. Equations

case	IVO/EVC	$P_{max,model}$ [atm]
1	25/165	57.4
2	45/185	52.4
3	65/205	47.4

Table 3. Model predicted values of peak in-cylinder pressure

40-43 can be solved simultaneously for experimental estimates of α and T_1 given values of $\bar{V}$, T_{ex} and V_1 from experiment. The results of these calculations are in Table 2. The engine speed for these conditions was 1800 rpm. Equation 31 can then be used to find the values of peak pressure predicted by the low-order model. These values are presented in Table 3.

By inspection of Tables 1 and 3 it can be seen that the experimental and model predicted values of peak pressure show reasonably good correlation. The simplicity and predictive capabilities of this low-order modeling approach make it a good candidate for model-based controller synthesis.

5 Linearization of Pressure Relation

Equation 31 can be further simplified by linearization about an operating point $(\bar{\alpha}, \bar{P})$, using the straightforward linear expansions for α and P:

$$\alpha_k = \bar{\alpha} + \tilde{\alpha}_k \tag{44}$$

$$P_k = \bar{P} + \tilde{P}_k \tag{45}$$

and the Taylor expansion of the term $P_{k-1}^{1/\gamma}$ taken to three terms:

$$P_{k-1}^{1/\gamma} \approx \bar{P}^{1/\gamma} + \tilde{P}_{k-1}\frac{\bar{P}^{(1-\gamma)/\gamma}}{\gamma} + \tilde{P}_{k-1}^2\frac{(1-\gamma)\bar{P}^{(1-2\gamma)/\gamma}}{2\gamma^2} \tag{46}$$

Applying these to 31, and neglecting the cross terms of fluctuations (i.e. $\tilde{\alpha_k}\tilde{P_k}, \tilde{\alpha_k}\tilde{\alpha_k}, \tilde{P_k}\tilde{P_{k-1}}, \tilde{P_k}\tilde{\alpha_{k-1}}\tilde{\alpha_k}$, etc) leads to:

$$\beta_k = -(c_{21}\bar{P}\beta_{k-1} + c_{22}\tilde{\alpha_k} + c_{23}\tilde{\alpha_{k-1}})/(c_{20}\bar{P}) \tag{47}$$

where β_k is the normalized difference between desired and actual pressure as:

$$\beta_k = \left(\frac{P_k - \bar{P}}{\bar{P}}\right) \tag{48}$$

and:

$$c_{20} = (1+\bar{\alpha})[c_{11}(c_1 + c_2\alpha) + c_{10}\bar{P}(1+\bar{\alpha}) + \bar{\alpha}P^{1/\gamma}\chi] \tag{49}$$

$$c_{21} = \frac{(1+\bar{\alpha})}{(c_1+c_2\bar{\alpha})^{-1}}\left[\begin{array}{l}\frac{c_{10}\bar{P}(1+\bar{\alpha}) + \frac{\bar{\alpha}P^{1/\gamma}\chi c_{14}}{\gamma}}{(c_1+c_2\bar{\alpha})} \\ + \frac{c_{15}\chi\bar{\alpha}P^{(1-\gamma)/\gamma}}{\gamma(1+\bar{\alpha})} + c_{13}\end{array}\right] \tag{50}$$

$$\begin{aligned} c_{22} = {} & (1+\bar{\alpha})\bar{P}(c_{13}c_2 + c_{10}\bar{P}) + (c_1 + c_2\bar{\alpha})(c_{12}c_2 + c_{11}\bar{P}) \\ & + (1+2\bar{\alpha})c_{14}\chi\bar{P}^{(1+\gamma)/\gamma} + (c_1 + 2c_2\alpha)c_{15}\chi\bar{P}^{1/\gamma} \end{aligned} \tag{51}$$

$$c_{23} = (1+\bar{\alpha})\bar{P}(c_{11}c_2 + c_{10}\bar{P}) + (c_1 + c_2\bar{\alpha})(c_{12}c_2 + c_{13}\bar{P}) \tag{52}$$

The question arises as to how well the linearized model corresponds to the nonlinear model. Figure 2 shows the open loop behavior of the linear model, Equation 47, with the nonlinear model, Equation 31. Note that very little is lost in the linearization.

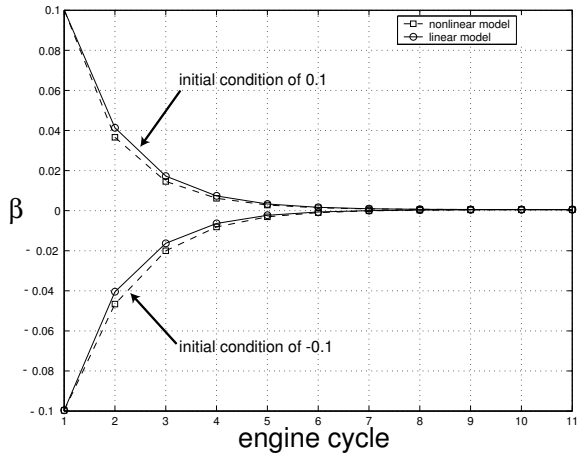

Figure 2. Open Loop Response of Linearized Model

5.1 Linear Transfer Function and State Space Formulations

Equation 47 can finally be written as a low-order discrete linear transfer function:

$$\frac{\beta(z)}{\alpha(z)} = -\frac{c_{22}/\bar{P} + c_{23}/\bar{P}z^{-1}}{c_{20} + c_{21}z^{-1}} \tag{53}$$

or in state space form:

$$x_{n+1} = Ax_n + Bu_n \tag{54}$$

$$y_n = Cx_n + Du_n \tag{55}$$

where:

$$A = \left[\begin{array}{cc} 0 & 0 \\ -\frac{c_{22}}{Pc_20} & -\frac{c_{21}}{c_{20}} \end{array}\right] \; B = \left[\begin{array}{c} 1 \\ -\frac{c22}{Pc_{20}} \end{array}\right] \; C = [0 \;\; 1] \; D = 0 \tag{56}$$

$$x_n = \begin{bmatrix} \tilde{\alpha}_{k-1} \\ \beta_{k-1} \end{bmatrix} \qquad u_n = \tilde{\alpha}_k \qquad y_n = \beta_k \tag{57}$$

6 LQR Controller synthesis

From the low-order linear model of HCCI combustion, a controller can be synthesized to track the desired in-cylinder peak pressure. In particular, a state feedback control law can be found with the form:

$$u_n = -Kx_n \tag{58}$$

which minimizes the cost function:

$$J = \sum x_n' Q x_n + u_n' R u_n + 2x_n' N u_n \tag{59}$$

This feedback control law is the standard linear quadratic regulator (LQR) with a controller output of α and full state feedback consisting of the previous cycles α and β, two easily attained values. With Q, R and N selected as:

$$Q = \begin{bmatrix} 0 & 0 \\ 0 & q \end{bmatrix} \qquad R = 1 \qquad N = \begin{bmatrix} 0 \\ 0 \end{bmatrix} \tag{60}$$

the cost function becomes:

$$J = \sum \left(q\beta_{k-1}^2 + \tilde{\alpha}_k^2 \right) \tag{61}$$

With this formulation, weights can be placed directly on both the output and input of the system, β and α, respectively.

7 Valve Timing Map

The control strategy presented uses the previous cycle's peak pressure, the desired peak pressure for the current cycle, and the value for α on the previous cycle to determine the desired α on the current cycle according to Equation 58. Before this can be implemented, however, a map from desired α to required valve timing (IVO/EVC) is necessary since it is in fact the valve timing that is controlled with the fully flexible VVA system. As presented in previous work (Caton *et al.* 2003) a set of IVO/EVC valve timings that span the load range of HCCI combustion can be defined which exhibit low emissions of both hydro-carbon and NO_x species. These operating points form a linear relation between IVO and EVC. Note that the conditions considered in Tables 1 - 3 do indeed have valve timings which follow this linear relation. A key feature of this linear relation is that all valve timings along it produce a fairly consistent combusting phasing. As noted previously, this is the reason why the constant volume combustion event is assumed to occur at this point. For the particular linear set of IVO and EVC valve timings considered here, combustion phasing initiation occurs at about 371 crank angle degrees.

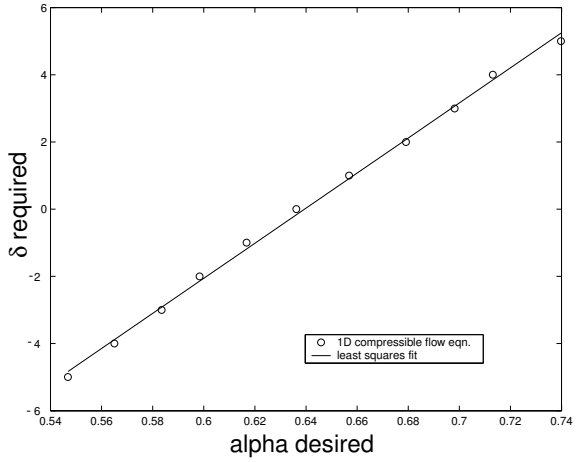

Figure 3. Relation between desired value of α and the required valve timing

In order to relate valve timings to values of α, a series of simulations with valve timings along this linear IVO/EVC set were completed. This relation is shown to be nearly linear about a mean operating point ($\bar{\alpha}$,$\bar{P}$) for absolute values of δ that do not exceed a value of 5, as shown in Figure 3. Here the value of δ corresponds to a deviation from the valve timing ($I\bar{V}O$,$E\bar{V}C$) corresponding to the point at which the model linearization was made about ($\bar{\alpha}$,$\bar{P}$). Mathematically this can be stated as:

$$IVO(\tilde{\alpha}) = I\bar{V}O + \delta = I\bar{V}O + f(\tilde{\alpha}) \tag{62}$$

$$EVC(\tilde{\alpha}) = E\bar{V}C + \delta = E\bar{V}C + f(\tilde{\alpha}) \tag{63}$$

While in fact this relationship does exhibit some dependence on the exhaust temperature due to the nature of the compressible flow equations, this is a fairly small effect and neglected for this implementation. Inverting this relationship, the valve timings can be obtained from knowledge of the desired α and the loop can be closed around the peak pressure in the cylinder. Figure 4 shows how the LQR controller is used in conjunction with the valve timing map in closed loop.

8 Controller Implementation on a 10-State Model of HCCI Combustion

The controller synthesized in the previous section can be implemented on a more complete model of HCCI combustion

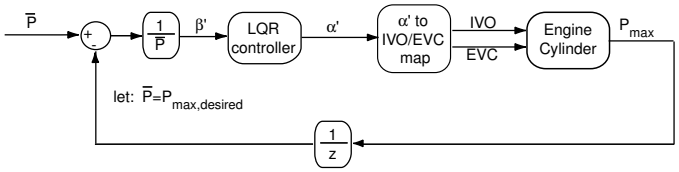

Figure 4. Block diagram of controller implementation

being developed in ongoing work (Shaver *et al.* 2004). This model is based on an open-system first-law analysis of both the in-cylinder and exhaust manifold gases, with steady state compressible flow relations used to model the mass flow through the intake and exhaust valves. This leads to a set of ten nonlinear differential equations for each of the model states: the crank angle, θ; the cylinder volume, V; the in-cylinder temperature, T; the concentrations of propane, $[C_3H_8]$, oxygen, $[O_2]$, Nitrogen, $[N_2]$, carbon dioxide, $[C_2O]$, water, $[H_2O]$; the mass in the exhaust manifold, m_e; and the internal energy of the product gases in the exhaust, u_e. Unlike the simplified model presented here, the more detailed model includes temperature dependence in the specific heats and the possibility of variable combustion phasing. In order to model HCCI combustion phasing in a simple and straightforward way, the model includes an integrated Arrhenius rate threshold approach described in detail in (Shaver *et al.* 2003). Figures 5 and 6 show the correlation between this modeling approach and experimental data taken from the single-cylinder research engine. It can be noted by inspection that the model results of combustion phasing and pressure correlate very well with experiment.

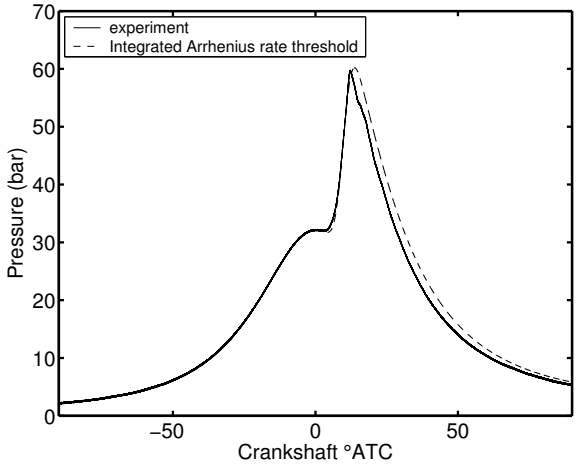

Figure 5. Model comparison with experiment: IVO @ 25deg., EVC @ 165

To test the controller strategy outlined in the paper, the LQR controller developed from the linear low-order model and the α

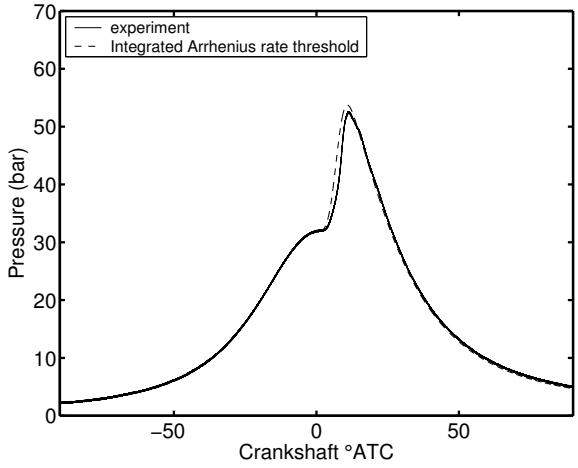

Figure 6. Model comparison with experiment: IVO @ 45deg., EVC @ 185

to IVO/EVC mapping methodology were applied in closed loop with the 10-state model. Figures 7 and 8 show the simulation results for peak pressure and combustion phasing as the desired peak pressure goes through a series of step changes. As expected, the combustion phasing is very consistent, with deviations less than one crank angle degree, once the controller begins to influence the system (i.e. after the first cycle). The closed loop response to the step changes in desired peak pressure are fairly rapid, and accurate after about 6 cycles. The specific response in desired peak pressure shown here is essentially arbitrary and controllers with more specific design objectives will be investigated in future work.

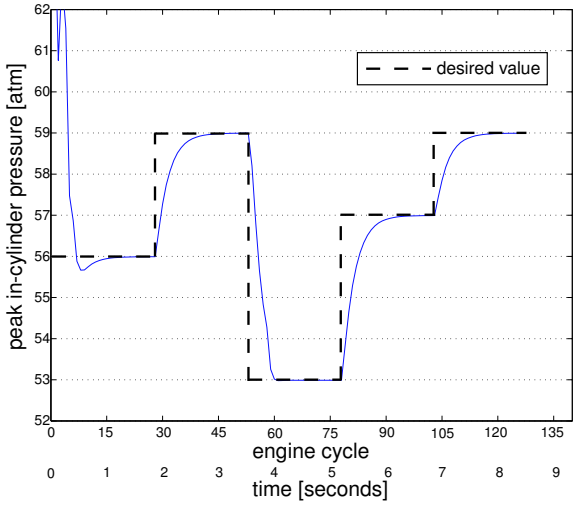

Figure 7. Simulation of tracking controller on 10-state model, dashed line: desired maximum pressure, solid line: actual peak pressure

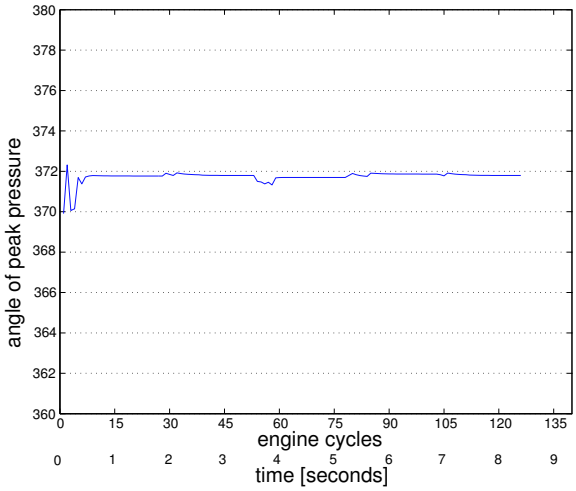

Figure 8. Simulation of tracking controller on 10-state model, crank angle location of peak pressure

9 Conclusion

While cycle to cycle dynamics and chemical kinetics make VVA-induced HCCI a complex process, a nonlinear low-order model that correlates well with experiment can nevertheless be developed. This was accomplished by splitting several key processes that occur during HCCI combustion into discrete steps. These include: constant pressure, adiabatic mixing of inducted reactants and re-inducted products from the previous cycle, isentropic compression up to the point where combustion initiates, constant volume combustion, isentropic volumetric expansion and isentropic exhaust. The resulting model can be linearized about an operating condition and used to synthesize controllers, such as the LQR controller developed here. Paired with a map from desired α to required IVO/EVC timing, this represents a complete approach for obtaining varying output loads at constant combustion phasing. A closed-loop simulation with a more complex 10-state HCCI model shows that despite the large number of simplifications, the control strategy is quite effective at tracking both the desired load and phasing. The results of this simulation suggest that the controller synthesis technique presented here is a good candidate for future experimental implementation.

10 Future Work

The next step in this work is the implementation of the controller strategy presented here on a single-cylinder research engine at Stanford. Following that, the next steps involve relaxing some of the restrictions of the current approach, including constant speed and constant combustion phasing. Although the selection of an IVO/EVC valve timing along a linear trajectory (as explained in Section 7) has been shown in previous experimental work to lead to fairly consistent phasing, this methodology is more empirical than perhaps it needs to be. Since previous modeling work has validated the use of an integrated Arrhenius rate to model combustion initiation, this value could be used to capture the relations among IVO, EVC and phasing in the form of a model. A model-based controller synthesis strategy can then by foreseen that enables variable combustion phasing to be used in conjunction with load control.

11 Acknowledgments

The authors would like to thank the Robert Bosch Corporation Research and Technology Center for their strong financial and technical support of this work. In particular, ongoing technical discussions with Dr. Jean-Pierre Hathout, Dr. Jasim Ahmed and Dr. Aleksandar Kojic have been highly appreciated and helpful.

REFERENCES

Caton, P.A., A.J. Simon, J.C. Gerdes and C.F. Edwards (2003). Residual-effected homogeneous charge compression ignition at low compression ratio using exhaust reinduction. *International Journal of Engine Research*.

Christensen, M., A. Hultqvist and B. Johansson (1999). Demonstrating the multi-fuel capability of a homogeneous charge compression ignition engine with variable compression ratio. *SAE paper 1999-01-3679*.

Kaahaaina, N.B., A.J. Simon, P.A. Caton and C.F. Edwards (2001). Use of dynamic valving to achieve residual-affected combustion. *SAE paper 2001-01-0549*.

Law, D., D. Kemp, J. Allen, G. Kirkpatrick and T. Copland (2001). Controlled combustion in an IC-engine with a fully variable valve train. *SAE paper 2001-01-0251*.

Martinez-Frias, Joel, Salvador M. Aceves, Daniel Flowers, J. Ray Smith and Robert Dibble (2000). HCCI engine control by thermal management. *SAE paper 2000-01-2869*.

Shaver, Gregory M., J. Christian Gerdes, Parag Jain, P.A. Caton and C.F. Edwards (2003). Modeling for control of HCCI engines. *Proceedings of the American Control Conference* pp. 749–754.

Shaver, Gregory M., Matthew Roelle and J. Christian Gerdes (2004). Multi-cycle modeling of HCCI engines. *Submitted to: First IFAC Symposium on Advances in Automotive Control*.

Tunestal, P., J-O Olsson and B. Johansson (2001). HCCI operation of a multi-cylinder engine. *First Biennial Meeting of the Scandinavian-Nordic Section of the Combustion Institute*.